

An embedded optical nanowire loop resonator refractometric sensor

Fei Xu¹, Valerio Pruneri^{2,3}, Vittoria Finazzi², and Gilberto Brambilla¹

¹Optoelectronics Research Centre, University of Southampton, Southampton SO17 1BJ, United Kingdom

fx@orc.soton.ac.uk

²ICFO-Institut de Ciències Fotoniques, Mediterranean Technology Park, 08860 Castelldefels (Barcelona), Spain

³Also with ICREA -Institució Catalana de Recerca i Estudis Avançats, 08010 Barcelona, Spain

Abstract: A novel refractometric sensor based on an embedded optical nanowire loop resonator is presented. The device sensitivity has been studied in two typical configurations and its dependence on the nanowire diameter and coating thickness determined.

©2008 Optical Society of America

OCIS codes: (060.2370) Fiber optics sensors; (230.5750) Resonators.

References and links

1. M. Adams, G. A. DeRose, M. Loncar, and A. Scherer, "Lithographically fabricated optical cavities for refractive index sensing," *J. Vac. Sci. Technol. B* **23**, 3168-3173 (2005).
2. C. Y. Chao, W. Fung, and L. J. Guo, "Polymer microring resonators for biochemical sensing applications," *IEEE J. Sel. Top. Quantum Electron.* **12**, 134-142 (2006).
3. N. M. Hanumegowda, C. J. Stica, B. C. Patel, I. White, and X. D. Fan, "Refractometric sensors based on microsphere resonators," *Appl. Phys. Lett.* **87**, 201107 (2005).
4. I. M. White, H. Oveys, X. Fan, T. L. Smith, and J. Y. Zhang, "Integrated multiplexed biosensors based on liquid core optical ring resonators and antiresonant reflecting optical waveguides," *Appl. Phys. Lett.* **89**, 191106 (2006).
5. I. M. White, H. Y. Zhu, J. D. Suter, N. M. Hanumegowda, H. Oveys, M. Zourob, and X. D. Fan, "Refractometric sensors for lab-on-a-chip based on optical ring resonators," *IEEE Sens. J.* **7**, 28-35 (2007).
6. L. M. Tong, J. Y. Lou, and E. Mazur, "Single-mode guiding properties of subwavelength-diameter silica and silicon wire waveguides," *Opt. Express* **12**, 1025-1035 (2004).
7. S. G. Leon-Saval, T. A. Birks, W. J. Wadsworth, P. S. J. Russell, and M. W. Mason, "Supercontinuum generation in submicron fibre waveguides," *Opt. Express* **12**, 2864-2869 (2004).
8. G. Brambilla, V. Finazzi, and D. J. Richardson, "Ultra-low-loss optical fiber nanotapers," *Opt. Express* **12**, 2258-2263 (2004).
9. M. Sumetsky, Y. Dulashko, J. M. Fini, A. Hale, and D. J. DiGiovanni, "The microfiber loop resonator: Theory, experiment, and application," *J. Lightwave Technol.* **24**, 242-250 (2006).
10. M. Sumetsky, "Optical fiber microcoil resonator," *Opt. Express* **12**, 2303-2316 (2004).
11. M. Sumetsky, Y. Dulashko, J. M. Fini, A. Hale, and D. J. DiGiovanni, "Demonstration of a microfiber loop optical resonator," in *Optical Fiber Communication Conference, 2005. Technical Digest. OFC/NFOEC* (2005), p. 3 pp. Vol. 5.
12. F. Xu, and G. Brambilla, "Manufacture of 3-D Microfiber Coil Resonators," *IEEE Photon. Technol. Lett.* **19**, 1481-1483 (2007).
13. F. Xu, and G. Brambilla, "Embedding optical microfiber coil resonators in Teflon," *Opt. Lett.* **32**, 2164-2166 (2007).
14. M. Sumetsky, Y. Dulashko, and M. Fishteyn, "Demonstration of a Multi-Turn Microfiber Coil Resonator," in *Optical Fiber Communication Conference and Exposition and The National Fiber Optic Engineers Conference*, OSA Technical Digest Series (CD) (Optical Society of America, 2007), paper PDP46. <http://www.opticsinfobase.org/abstract.cfm?URI=OFC-2007-PDP46>.
15. G. Brambilla, F. Xu and X. Feng, "Fabrication of optical fibre nanowires and their optical and mechanical characterisation," *Electron. Lett.* **42**, 517-518 (2006).
16. F. Xu, and G. Brambilla, "Demonstration of optical microfiber coil resonator refractometric sensor," submitted.
17. F. Xu, P. Horak, and G. Brambilla, "Optical microfiber coil resonator refractometric sensor," *Opt. Express* **15**, 7888-7893 (2007).
18. F. Xu, P. Horak, and G. Brambilla, "Optical microfiber coil resonator refractometric sensor: erratum," *Opt. Express* **15**, 9385-9385 (2007).

19. M. S. Dinleyici, and D. B. Patterson, "Vector modal solution of evanescent coupler," *J. Lightwave Technol.* **15**, 2316-2324 (1997).
 20. D. Marcuse, F. Ladouceur, and J. D. Love, "Vector Modes of D-Shaped Fibers," *IEEE Proc. J. Optoelectronics* **139**, 117-126 (1992).
 21. C. Y. Chao, and L. J. Guo, "Design and optimization of microring resonators in biochemical sensing applications," *J. Lightwave Technol.* **24**, 1395-1402 (2006).
 22. G. M. Hale, and M. R. Querry, "Optical-Constants of Water in 200-Nm to 200-Mum Wavelength Region," *Appl. Opt.* **12**, 555-563 (1973).
-

1. Introduction

Optical microresonators based on evanescent-field coupling have recently attracted a great deal of attention as biological and/or chemical sensors; microspheres, photonic crystals, and microrings have been widely investigated for this applications [1-5] because they can provide small size, high sensitivity, high selectivity, and low detection limits; in particular they can provide large evanescent fields for high sensitivity, high Q-factors for low detection limits, and corresponding small resonant bandwidths for good wavelength selectivity. Recently, microresonators based on subwavelength-diameter optical fibre nanowire have emerged as ideal sensor elements because of their low cost, low loss, and very large evanescent fields [6-8]. Self-coupling loop resonators and 3D microcoil resonators have been demonstrated [9-14]. These fibre microresonators do not exhibit the input/output coupling problems experienced in other high-Q resonators because the fibre pigtailed at the extremities of the resonator launch and collect the totality of the light. However, in free space the fabrication of these devices with high reliability is challenging due to problems of stability, degradation, and cleanness [15]. Coating is an elegant way to solve these issues; yet, the determination of the coating thickness is a challenging issue because a thick coating layer will limit the sensitive evanescent field, while a thin layer does not provide an appropriate protection to the device. Consequently to the development of 3D microcoil resonators [10, 12] in Teflon [13] and in low index liquid [14], a refractometric sensor based on a coated optical nanowire microcoil resonator has been investigated and demonstrated [16-18]. The device, called coated all-coupling nanowire microcoil resonator (CANMR), had a sensitivity as high as 700 nm/RIU and a refractive index resolution as low as 10^{-7} . Compared to the 3D resonator, the loop resonator has a simpler structure and can be manufactured in an easier way. In this paper, the possibility to exploit an embedded self-coupling loop resonator for sensing applications is investigated. Its performance as a function of the geometry (nanowire diameter and coating thickness) is analysed.

2. Fabrication

An embedded nanowire loop resonator (ENLR) can be fabricated as shown in Fig. 1(a): two substrates are fabricated with disposable materials (blue) such as PMMA (PolyMethylMethAcrylate) and coated with a thin layer of a low-loss low-refractive-index polymer such as Teflon or UV375 (green); next, the self-coupling nanowire loop resonator (red) with a 1 mm diameter is manufactured on one of the substrates; then the other substrate is placed on top of the nanowire resonator. The use of a thick substrate allows to easily handle thin coating layers. The whole system is subsequently coated by a thick polymer layer and at last the expendable materials are removed (for example, PMMA can be dissolved in Acetone), leaving a thin layer of low refractive index material on the nanowire.

The final device is shown in Fig. 1(b): a very thin polymer layer covers the loop of the ENLR while a thick coating deposit is used to fix the two fibre pigtailed. The ENLR is a compact and robust device with two sides exposed to the liquid to sense. The embedded nanowire has a considerable fraction of its mode propagating outside the embedding medium both in the in the upper and lower areas, thus any change in the analyte properties reflects in a change of the mode properties at the ENLR output. Since the ENLR is fabricated from a single tapered optical fiber, light can be coupled into the sensor with essentially no insertion loss, a huge advantage over other types of resonator sensors. Fig 2(b) and 2(c) are not drawn

to scale for clarity because the value of d is orders of magnitude smaller than the nanowire diameter.

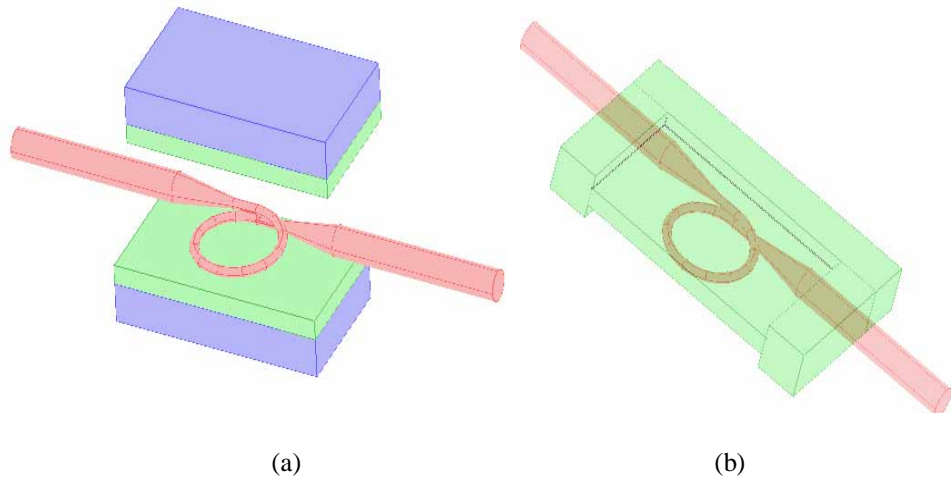


Fig. 1. (a) Schematic of the manufacturing process of an ENLR.(b) the final structure of the ENLR.

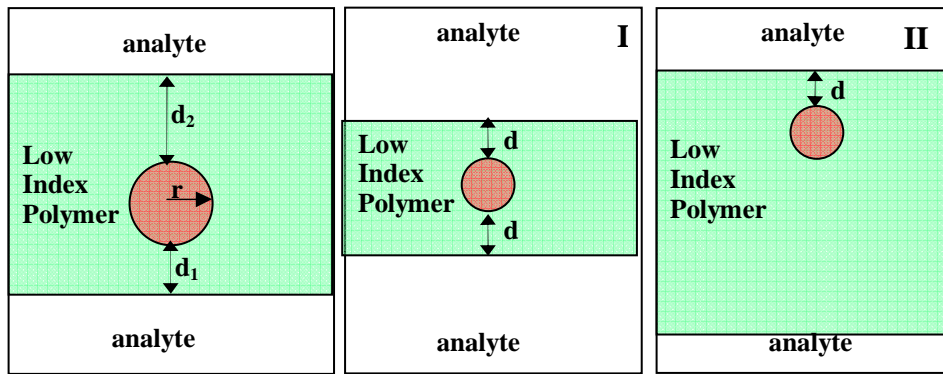


Fig. 2. Cross-section of the ENLR, (I) $d_1=d_2=d<1\mu\text{m}$, (II) $d_1\rightarrow\infty$ and $d_2=d<1\mu\text{m}$

3. Effective Index of the ENLR

Assuming continuous-wave (CW) input, a change of the analyte refractive index will lead to a change of the effective index n_{eff} of the propagating mode, thereby shifting the mode relative to the resonance and thus modifying the transmission spectrum. The transmission coefficient T can be easily evaluated using the coupled mode equations with results analogous to those of a single-loop resonator [9]; if $\beta = 2\pi n_{eff} / \lambda$ is the propagation constant, α the loss coefficient, and $K = \kappa L$ the coupling parameter for coupling coefficient κ and nanowire loop length L , the resonances condition is [9]:

$$\beta_n = (2n+1)\pi / (2L), \quad (1)$$

where n are integer numbers.

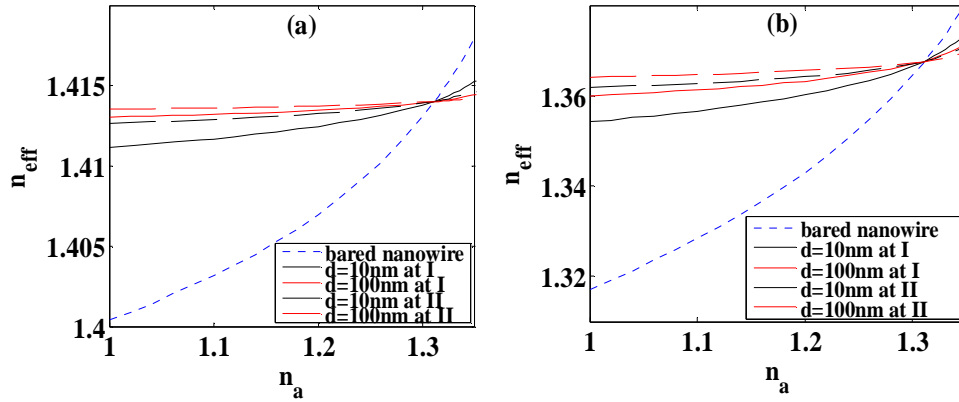


Fig. 3. Dependence of the effective index of a coated nanowire n_{eff} on the index of the analyte n_a for $n_t=1.311$, $n_c=1.451$, $r=500$ nm, bared nanowire (blue dotted line), $d=10$ nm (black line) and 100 nm (red) for small coating thicknesses (case I: solid line) and infinitely thick layer on one side (case II: dashed). The wavelength of the propagating mode is (a) $\lambda=600$ nm, (b) $\lambda=970$ nm.

Because of the interface with the analyte, the mode propagating in the coated fiber nanowire experiences a refractive index surrounding which is strongly affected by the analyte. The ENLR cross-section is shown in Fig. 2; the mode properties are particularly affected by three important parameters: the nanowire radius r and the coating thicknesses d_1 and d_2 in the upper and lower layers. When one of the distances d_1 and d_2 is very large, the device resembles the case of a conventional D-shaped fiber [19, 20]. Two typical cases are investigated, (I) $d_1=d_2=d<1\mu\text{m}$ and (II) $d_1\rightarrow\infty$ and $d_2=d<1\mu\text{m}$; the effective index n_{eff} of the fundamental mode propagating in the optical fibre nanowire was evaluated by a finite element method with the commercial software COMSOL3.3. Figure 3 shows the dependence of n_{eff} on the analyte refractive index n_a assuming the refractive index of the nanowire and of the embedding low refractive index polymer (Teflon) to be $n_c=1.451$ and $n_t=1.311$, respectively. While r is assumed to be 500 nm, two values for d are considered: 10 nm and 100 nm. The fundamental mode is the one with the largest propagation constant and the only mode that is well confined in the vicinity of the nanowire [19]. Generally, n_{eff} increases with n_a , and increases more quickly with smaller d in I and II since in this case a larger fraction of the mode is propagating in the analyte. n_{eff} in I is larger than in II when $n_a<n_t$, and n_{eff} in I is smaller than in II when $n_a>n_t$. If $n_a=n_t$, the propagating light does not experience the boundary between Teflon and the analyte solution, and therefore n_{eff} is independent of the Teflon thickness d , as seen in Fig. 3. The dependence for the bare nanowire is presented for comparison.

4. Sensitivity

Two sensing approaches are most commonly used: homogeneous sensing and surface sensing [21]. In homogeneous sensing, the device is typically surrounded by an analyte solution, which can be regarded as the top cladding of the waveguide. The homogeneously distributed analyte in the solution will modify the bulk refractive index of the solution. In surface sensing, the optical device is pretreated to have receptors or binding sites on the sensor surfaces, which can selectively bind the specific analyte [21]. Here we only discuss the conceptually simpler case of homogeneous sensing.

When the propagation constants β_n is uniform, the homogeneous sensitivity S obtained by monitoring the shift of the resonant wavelength λ_0 corresponding to β_n can be defined as [21]

$$S = \frac{\partial \lambda_0}{\partial n_a} = \frac{\partial \lambda_0}{\partial n_{eff}} \frac{\partial n_{eff}}{\partial n_a} = \frac{\lambda_0}{n_{eff}} \frac{\partial n_{eff}}{\partial n_a} \quad (2)$$

This can be considered as the device transfer function. Because water is the solvent for most biological analytes and the absorption of water at long wavelengths is high [22], we calculated the sensitivity near $n_a=1.332$ at short wavelengths (600 nm and 970 nm). Figure 4 shows the dependence of S on the nanowire radius r for different d at I and II. S increases when d decreases or λ increases in accordance with the results of Fig. 4. Decreasing the nanowire radius r also increases S because this increases the fraction of the mode field inside the fluidic channel. S reaches 500 nm/RIU (where RIU is refractive index unit) at $r \approx 200$ nm for $\lambda=600$ nm and 700 nm/RIU at $r \approx 300$ nm for $\lambda=970$ nm. This is higher than in most microresonator sensors.

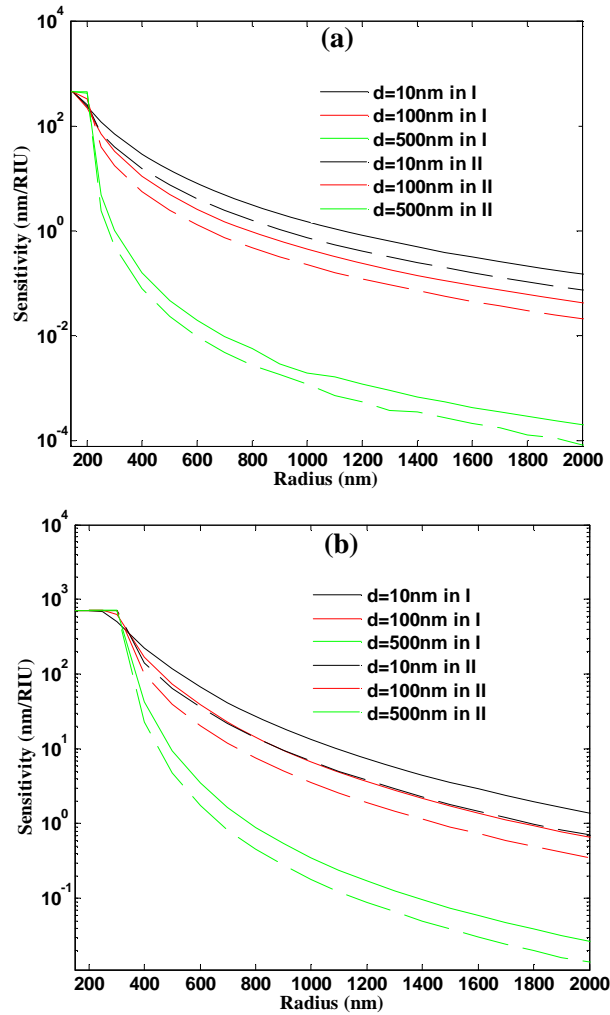


Fig. 4. Sensitivity of the ENLR versus nanowire radius for (a) $\lambda=600$ nm and (b) $\lambda=970$ nm and for different values of d in I (solid line) and II (dashed). Here, $n_a=1.332$, $n_i=1.311$, and $n_c=1.451$.

At the same wavelength and diameter of microfiber, the sensitivity in case I (two sensing surfaces) is larger than in case II (one sensing surface), because of the larger overlap between the evanescent field propagating in the nanowire and the analyte. For even smaller values of r , the sensitivity reaches a plateau because the fundamental mode is no longer well confined and most of the evanescent field is in the analyte. The change of n_{eff} becomes linearly dependent on n_a , the derivative in the last term of equation 2 reaches a uniform value and the sensitivity reaches a plateau.

In our simulation, we assume uniform β and loss, which is difficult to realize in real cases. For example, where the nanowire loop closes, the ENLR height doubles, the overlay thickness can change, the two device/analyte interfaces are not parallel, and d and β are not uniform. Additionally, when d is as small as 10 nm, the refractive index is close to the value of the surface refractive index, rather than to the bulk refractive index. For theoretical estimation, d , β and n can be assumed to represent the averaged values over the nanowire loop and it is still possible to assume that they are uniform along the device length.

The sensitivity predicted for the ENLR sensors is the same as the sensor based on a 3D resonator [17] because the mode propagating in the microfiber experiences the same effective refractive index changes. Still, the manufacture of the embedded sensor is not easier than that of the nanowire without support, but the protected device is clearly advantageous.

5. Conclusion

In summary, we have investigated a novel refractometric sensor in the form of an embedded optical nanowire loop resonator, which is strong and extremely compact. The manufacture method was presented and discussed. Two different sensor configurations have been considered and the device sensitivity has been evaluated for different sensor geometries. For optimized designs, sensitivities up to 700 nm/RIU can be achieved.

Acknowledgments

The authors gratefully acknowledge the help of Dr. N. Broderick with the software package COMSOL, initiating discussions with Prof. D. J. Richardson and financial support by the EPSRC. GB acknowledges the Royal society for his research fellowship.